Catalysis Letters 29 (1994) 133–143

Ethylene dimerization over a model Sn/Pt(111) catalyst

János Szanyi and Mark T. Paffett[1]

Chemical Science and Technology Division, Los Alamos National Laboratory,
MS G740, Los Alamos, NM 87545, USA

Received 13 May 1994; accepted 15 August 1994

The dimerization reaction of ethylene was studied over Pt(111) and $(\sqrt{3}\times\sqrt{3})$R30°-Sn/Pt(111) model catalysts at moderate pressures (20–100 Torr). The catalyst surfaces were prepared and characterized in a UHV surface analysis system and moderate pressure catalytic reactions were conducted with an attached batch reactor. The overall catalytic activity of the $(\sqrt{3}\times\sqrt{3})$R30°-Sn/Pt(111) surface alloy for C_4 products was slightly higher than that at Pt(111). In addition to the dimerization reaction, hydrogenolysis of ethylene to propane and methane was also observed, with the $(\sqrt{3}\times\sqrt{3})$R30°-Sn/Pt(111) surface alloy less active than Pt(111). Among the C_4 products, butenes and *n*-butane were the major components. Carbon buildup was observed to be significant above 500 K with the $(\sqrt{3}\times\sqrt{3})$R30°-Sn/Pt(111) surface alloy much more resistant than Pt(111). The dimerization of ethylene was not eliminated by the presence of surface carbonaceous deposits and even at significant surface coverages of carbon the model catalysts exhibited significant activities. The results are discussed in terms of the surface chemistry of ethylene and the previously reported catalytic reactions of acetylene trimerization and *n*-butane hydrogenolysis at these surfaces.

Keywords: ethylene; dimerization; Pt(111); Sn/Pt(111); UHV

1. Introduction

The catalytic conversion of hydrocarbons into more desirable end-products is central to many large scale industrial processes. For many of the supported catalysts used in these processes the primary metal catalyst is platinum because of its well known activity for C–C and C–H bond activation. The product distributions in these reactions can be altered by the additional metal components and the nature of the support. Bimetallic catalysts are widely utilized in hydrocarbon transformation reactions because of their improved activities and/or selectivities toward the desired products or their increased resistance toward catalyst poisons as compared to the monometallic catalysts [1].

It has been demonstrated [2–4] that it is possible to prepare ordered surface

---

[1] To whom correspondence should be addressed.

alloys that incorporate Sn into the surface plane of the single crystal template for a number of group VIII transition metals (e.g., Ni, Pd, Pt, Rh, Ru). The alloying of Sn with these transition metals results in very interesting surface and catalytic chemistry [6–10]. For example, the rate of CO oxidation was significantly enhanced at the $\Theta_{\mathrm{Sn}} = 0.50$ c(2 × 2)-Sn/Pd(100) surface alloy in comparison to Pd(100) [6]. Furthermore, the activity and selectivity patterns were dramatically altered in *n*-butane hydrogenolysis at both the p(2 × 2) and the ($\sqrt{3} \times \sqrt{3}$)R30°-Sn/Pt(111) surface alloys [7]. Our overall motivation has been to prepare and utilize ordered surface alloys that inherently only have certain ensembles (contiguous transition metals atoms). Through this control of catalytic reaction site chemistry improved catalytic surfaces have been demonstrated using this catalytic surface science perspective [6–10]. It remains the synthetic challenge to exploit these details in preparing real world supported transition bimetallic catalysts.

In this paper we report the results of a continuing effort to explore the catalytic properties of these model bimetallic systems. We have conducted catalytic experiments at elevated pressures with an ethylene/hydrogen gas mixture over Pt(111) and ($\sqrt{3} \times \sqrt{3}$)R30°-Sn/Pt(111) model catalysts surfaces. This work has close parallels to our related work on the di- and trimerization of acetylene and in *n*-butane hydrogenolysis over the same surfaces that are presented in other publications [7,9]. The changes in activity and selectivity patterns as functions of reaction temperature, reactant partial pressure and reaction time are all examined in the context of previous UHV characterization studies and prior batch catalytic reaction chemistry.

2. Experimental

The experiments were carried out in an elevated pressure reactor–ultrahigh vacuum (UHV) surface analysis system that has been described in detail previously [2,11]. Briefly, the UHV chamber with a base pressure of 3×10^{-10} Torr is equipped with basic surface analytical techniques (Auger electron spectroscopy (AES), X-ray photoelectron spectroscopy (XPS), low energy ion scattering spectroscopy (LEISS) and low energy electron diffraction (LEED)) and gas and metal dosing facilities. The elevated pressure reaction cell, which can be operated in the pressure range of 10^{-9}–10^{3} Torr is attached to the UHV system through a gate valve. The Pt(111) crystal was mounted to the sample holder rod via tungsten heating wires spotwelded to the edge of the crystal, which allowed the heating of the sample to 1200 K. The temperature of the crystal was monitored by using a chromel/alumel thermocouple spotwelded to the edge of the sample. The catalyst was cleaned by cycles of Ar^{+} sputtering/oxidation/anneal until no detectable impurities were seen. The surface cleanliness and composition were verified by AES and the long range surface structure was determined by LEED. The surface alloy samples were prepared by vapor deposition of a certain amount of Sn onto the clean Pt(111) surface at room temperature, followed by an anneal to 1000 K. Extensive characterization studies on the surface alloys of Sn/Pt(111) have been reported elsewhere [2,5] and are described briefly, where necessary, in the following sections. After cleaning and preparing the catalyst samples the crystal was transferred into the reactor chamber for elevated pressure catalytic experiments. A typical reaction run was carried out as follows: after introduction of the ethylene and hydrogen gases a sufficient amount of time was allowed to ensure the mixing of the reactant gases and then the catalyst temperature was raised quickly to the desired level and kept at that value (±2 K) for a given period of time. The reaction was rapidly quenched by cooling the catalyst. This was followed by the condensation of the gases into a liquid nitrogen cooled metal bulb. The gas analysis was carried out with a gas chromatograph (GC) equipped with a flame ionization detector and corrections for methane sensitivity (which is not trapped at 77 K) were conducted through comparison to standard gas mixture (C_1–C_6 mixture, Scott Specialty, #220). A Porapak N column was used for gas separation at 423 K. After each catalytic experiment the reactor cell was pumped down and then the sample was transferred back into the UHV chamber for surface analysis.

Research purity gases (Matheson) of ethylene and hydrogen were used without further purification. The turnover frequencies (TOFs – molecules produced per surface site per second) reported represent initial reaction rates obtained at low conversion levels ($<5\%$). Activities were linear over various reaction time intervals ranging from several minutes to an hour. The activities and surface coverages (in monolayer units (ML)) are reported with respect to the Pt(111) surface atom density of 1.505×10^{15} atoms cm^{-2}. The sample was a polished disk ~ 1 cm in diameter 1 mm thick. The $(\sqrt{3} \times \sqrt{3})R30°$-Sn/Pt(111) surface alloy data are reported using the same number of surface metal atoms (not corrected for loss of surface Pt atoms).

3. Results

3.1. TEMPERATURE DEPENDENCE

The activities of the $(\sqrt{3} \times \sqrt{3})R30°$-Sn/Pt(111) model catalyst and Pt(111) were determined in the ethylene + hydrogen reaction over the temperature range 425–575 K using an $H_2/C_2H_4 = 10$ reactant gas mixture at a total pressure of 22.0 Torr. The activities of the two catalysts as a function of reaction temperature are displayed in figs. 1 and 2 for Pt(111) and $(\sqrt{3} \times \sqrt{3})R30°$-Sn/Pt(111), respectively, in Arrhenius form. The product hydrocarbons detected over both surfaces are the dimerization products of ethylene (butane and butene, denoted as C_4 products) and the hydrogenolysis products, propane and methane. Under our experimental conditions part of the initially present ethylene was hydrogenated to ethane, however the GC analysis procedure applied in this work did not allow the quantitative separation of these two C_2 hydrocarbons. On both surfaces, the C_4

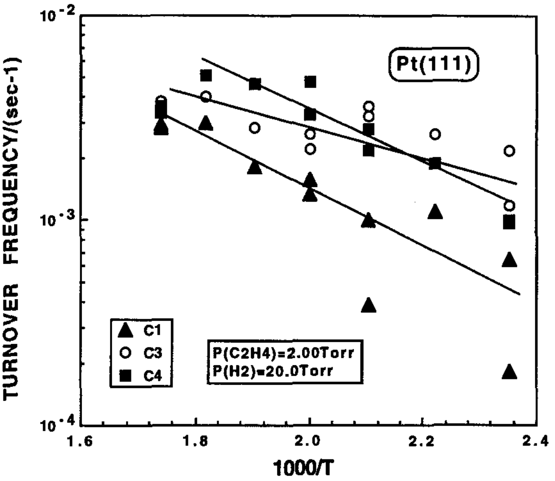

Fig. 1. Turnover frequency for various products of the C_2H_4/H_2 reaction mixture versus inverse temperature at Pt(111). The total pressure was 22.0 Torr and the the partial pressures were 2.00 Torr for ethylene and 20.0 Torr for hydrogen.

hydrocarbons are produced at approximately the same rate, the alloy surface being slightly more active than the Pt(111). Over both catalysts the C_4 formation rates go through maxima in the temperature range of 500–520 K and then, above this temperature region, the formation rates of C_4 hydrocarbons decrease with increasing temperature. The apparent activation energies calculated for the low temperature linear portion of the Arrhenius plot are essentially identical on the two surfaces, i.e. it is 7.5 ± 1 kcal/mol. Both the propane and methane formation rates (principally from hydrogenolysis reactions) are significantly higher over the

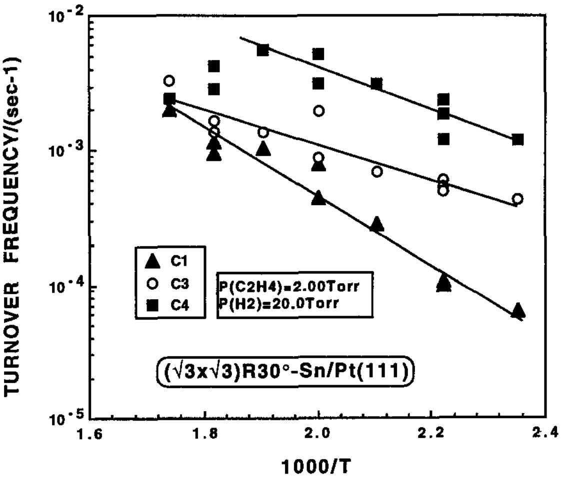

Fig. 2. The same plot as in fig. 1 except at the ($\sqrt{3} \times \sqrt{3}$)R30°-Sn/Pt(111) surface alloy.

Pt(111) surface than on the ($\sqrt{3} \times \sqrt{3}$)R30°-Sn/Pt(111) surface alloy. The apparent activation energies for methane and propane formations are ~ 3.5 kcal/mol higher for the ($\sqrt{3} \times \sqrt{3}$)R30°-Sn/Pt(111) surface alloy than for the clean Pt(111). The apparent activation energies for methane formation are 6.6 ± 1 kcal/mol for Pt(111) and 10.9 ± 1.5 kcal/mol for the alloy surface and for propane formation the corresponding values are 2.8 ± 1 kcal/mol for Pt(111) and 6.2 ± 1 kcal/mol for ($\sqrt{3} \times \sqrt{3}$)R30°-Sn/Pt(111). On the Pt(111) surface in the low temperature region propane is the major product while over the alloy surface C_4 hydrocarbons are produced with the highest turnover frequencies over the entire temperature range studied.

The carbon buildup, expressed as both the C(273 eV)/Pt(66 eV) Auger signal intensity ratio and in C coverage (monolayer units) following the calibration of Sachtler and Somorjai [12] over the two surfaces as a function of reaction temperature is shown in fig. 3. Below 500 K both surfaces are practically carbon free and carbon starts to build up only $\geqslant 500$ K. At higher temperatures the carbon buildup is very fast on the Pt(111) surface, however it is dramatically lower over the ($\sqrt{3} \times \sqrt{3}$)R30°-Sn/Pt(111) surface alloy. This has been noted previously in studies of ethylene adsorption and *n*-butane hydrogenolysis reactions on Sn/Pt(111) surface alloys [7,13]. The turn-on temperatures for carbon buildup correlate with the observed temperature where the dimerization rate rolls over.

3.2. HYDROGEN PARTIAL PRESSURE DEPENDENCE

The production of methane, propane and C_4 hydrocarbons from an ethylene/hydrogen mixture in which the hydrogen partial pressure was varied was followed at a 500 K reaction temperature. The ethylene partial pressure was held constant at 2.00 Torr and the total pressure was 102.0 Torr with neon used as the balance

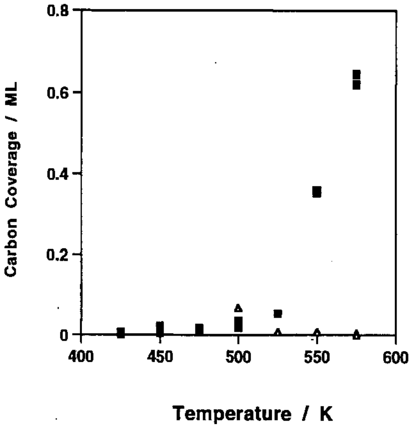

Fig. 3. Post-reaction carbon buildup plotted as coverage (after calibration of ref. [17]) versus temperature at (■) Pt(111) and at the (△) ($\sqrt{3} \times \sqrt{3}$)R30°-Sn/Pt(111) surface alloy. Reaction conditions as in figs. 1 and 2.

gas. The turnover frequencies for all three products of interest are displayed in figs. 4 and 5 for Pt(111) and ($\sqrt{3} \times \sqrt{3}$)R30°-Sn/Pt(111), respectively, as a function of hydrogen partial pressure. The activity patterns are very similar for the two surfaces. Over Pt(111) at hydrogen pressures lower than 5 Torr the C_4 hydrocarbon formation rate is positive first order in hydrogen partial pressure and then it rolls over at $P_{H_2} > 20$ Torr and decreases with increasing hydrogen pressure. The formation rate of propane follows closely that of C_4 hydrocarbons, although at 5 Torr hydrogen pressure it is lower than the turnover frequency for C_4 hydrocarbon formation and at $P_{H_2} = 100$ Torr it is higher than the C_4 formation rate. The turnover frequency for methane production is positive order in hydrogen pressure up to 50 Torr and then above this pressure it rolls over and decreases with increasing hydrogen pressure. Note that the turnover frequencies for methane formation are lower than that for propane production over the entire hydrogen pressure range studied. (In the low hydrogen pressure region, $P_{H_2} < 5$ Torr, the turnover frequency for methane formation is comparatively low at $\leqslant 1 \times 10^{-4}$ s^{-1}, it then increases to $\sim 1 \times 10^{-3}$ s^{-1} with increasing P_{H_2} and reaches a maximum value at 1×10^{-3} s^{-1} for 50 Torr P_{H_2}. The rate then decreases with further increases of PH_2.) The formation rate of propane over the Pt(111) surface does not change significantly over the entire hydrogen pressure region studied. For the ($\sqrt{3} \times \sqrt{3}$) R30°-Sn/Pt(111) surface alloy, the C_4 hydrocarbon production rate is similar to that observed on Pt(111), in that it is positive first order in hydrogen pressure at $P_{H_2} < 20$ Torr and rolls over and decreases with increasing hydrogen partial pressure. The TOFs for propane formation follow those of C_4 hydrocarbons at hydrogen pressures below 20 Torr but at higher hydrogen pressures propane formation remains constant and does not decrease as seen for the C_4 hydrocarbons. The

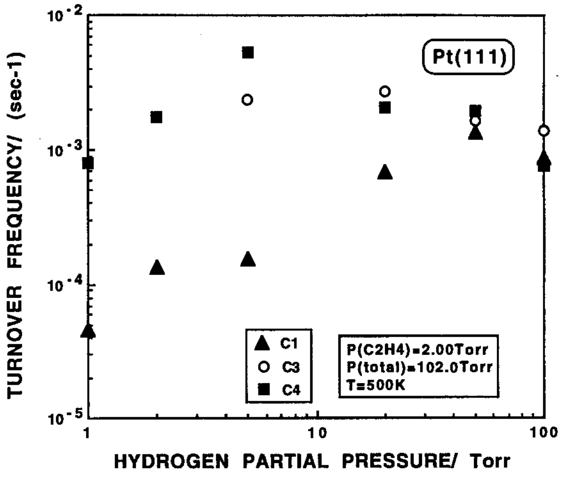

Fig. 4. Turnover frequency for various products of the C_2H_4/H_2 reaction mixture versus hydrogen partial pressure at Pt(111). The total pressure was 102.0 Torr and the partial pressure of ethylene was 2.00 Torr.

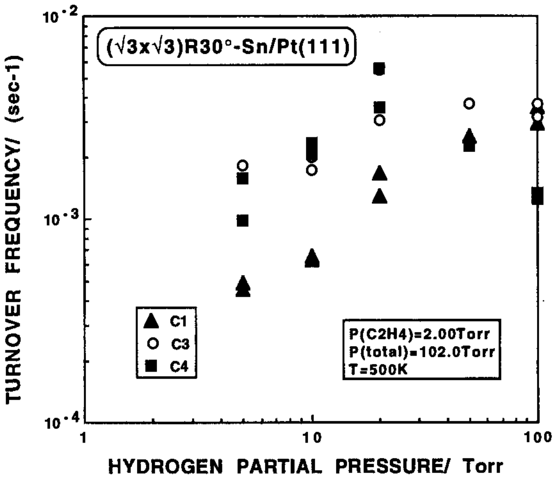

Fig. 5. Same as in fig. 4 except for the ($\sqrt{3} \times \sqrt{3}$)R30°-Sn/Pt(111) surface alloy.

methane formation rate is positive order in hydrogen partial pressure over the entire hydrogen pressure range studied and is below the production rate of propane up to the highest hydrogen partial pressure of 100 Torr.

4. Discussion

Under the experimental conditions of this study four reaction routes are available for hydrocarbon molecules present in the reactor. The ethylene molecules can dimerize to produce C_4 hydrocarbons or undergo hydrogenation to form ethane. The C_4 hydrocarbons, the primary products in ethylene dimerization reaction, can undergo hydrogenolysis, which results in the formation of propane and methane. And finally, the complete decomposition of any of the hydrocarbons present can produce surface carbonaceous residues. The results demonstrate that all four of these processes are operational but their contributions in determining the final product distributions are strongly influenced by the reaction conditions applied (H_2/C_2H_4 ratio, reaction temperature). It is evident that the dimerization of ethylene readily proceeds over both of the surfaces producing butane with fairly high turnover frequencies. No trimerization products were seen except at very high C_2H_4/H_2 ratios (>4), where trace amounts of C_6 hydrocarbons were detected. This is in contrast to what we have found for acetylene reactions over the same two surfaces under identical reaction conditions [9]. There are two major differences between acetylene and ethylene reactions on these two catalysts. First, acetylene di- and trimerizes over both Pt(111) and ($\sqrt{3} \times \sqrt{3}$)R30°-Sn/Pt(111) surfaces producing C_4 and C_6 hydrocarbons. Second, no hydrogenolysis products (C_1, C_3, and C_5) are formed in the acetylene reactions except at extreme reaction conditions (at the highest reaction temperature and the highest hydrogen pressure), where trace amounts of methane and propane were seen. During ethylene reactions no trimerization products were seen and methane and propane as the hydrogenolysis products were formed with high turnover frequencies. These reaction differences probably arise from the different reactivities of ethylene and acetylene toward the Pt(111) and ($\sqrt{3} \times \sqrt{3}$)R30°-Sn/Pt(111) surfaces [13,14]. The adsorbate–surface interaction is stronger for an acetylene molecule than for ethylene. This is readily noted in the large differences reported for the desorption temperatures of these two unsaturated C_2 hydrocarbons from the Pt(111) and Sn/Pt(111) alloy surfaces [13,14]. Ethylene adsorbs molecularly on the Pt(111) surface and exhibits a desorption peak maximum centered at 285 K with approximately 40% of the molecules decomposing following desorption of a saturation coverage. In contrast, most of the acetylene adsorbed at low temperatures (<120 K) does not desorb molecularly from this surface but rather decomposes to form surface carbon and hydrogen. The adsorption strengths for both ethylene and acetylene molecules are weakened by the presence of Sn in the surface layer of Pt(111) and, furthermore, they decrease with increasing Sn coverage [14]. For example, the desorption peak temperature of a saturation coverage of ethylene is some 45 K lower on the p(2 × 2)-Sn/Pt(111) surface than it is on the Pt(111) surface and it further decreases to ~ 185 K on the ($\sqrt{3} \times \sqrt{3}$)R30°-Sn/Pt(111) surface. Acetylene desorbs from the ($\sqrt{3} \times \sqrt{3}$)R30°-Sn/Pt(111) surface alloy at a desorption peak temperature of 365 K, which is notably higher (by ~ 180 K) than that observed for ethylene desorption. These very large differences in adsorption strengths between these two C_2 hydrocarbon molecules are suggested to be responsible for the vastly different product distributions and activities. At Pt(111) and the ($\sqrt{3} \times \sqrt{3}$)R30°-Sn/Pt(111) surface alloy acetylene is suggested to predominately produce an unsaturated surface species (for example, metallocyclopentadiene), which can be hydrogenated off from the surface as mono- and diolefinic hydrocarbons. Furthermore, these unsaturated surface intermediates are available to react with another acetylene molecule, thus producing chain and ring C_6 hydrocarbons. Conversely, the degree of saturation is suggested to be significantly higher in the intermediates produced from ethylene reaction; therefore their reactivities toward addition of another ethylene molecule are much lower and almost exclusively saturated C_4 hydrocarbons are produced. These butane molecules, however, are very capable of taking part in further reactions, namely hydrogenolysis. The hydrogenolysis of *n*-butane which were produced in the primary dimerization reaction results in the formation of propane and methane. A more complete description of the hydrogenolysis of *n*-butane is described in a related publication [7]. An in situ vibrational spectroscopic study would clearly provide insightful evidence for the existence of these proposed surface intermediates.

Over both Pt(111) and ($\sqrt{3} \times \sqrt{3}$)R30°-Sn/Pt(111) surfaces the Arrhenius plots roll over at reaction temperatures near 500 K. Two effects are suggested to be responsible for this roll over. The first contributing factor is the temperature dependence of the ethylene coverage on these surfaces. The depletion of the ethylene coverage at high reaction temperatures can result in the decrease of the dimerization reaction rate. The second contributing factor is the accelerated carbon buildup on the surface at these high reaction temperatures which decreases the number of available active sites by blocking adsorption sites for ethylene molecules. A very good correspondence between the temperatures where the dimerization activities roll over and the observed carbon buildup suggests that the second factor is responsible for decreased catalytic activities at temperatures higher than 500 K.

The TOFs for methane and propane are higher over the Pt(111) surface than at the $(\sqrt{3} \times \sqrt{3})$R30°-Sn/Pt(111) surface alloy. This is in good agreement with the results of our previous study on *n*-butane hydrogenolysis over the same two surfaces. We have reported that the *n*-butane hydrogenolysis rates were about an order of magnitude lower over the $(\sqrt{3} \times \sqrt{3})$R30°-Sn/Pt(111) surface than on the Pt(111). It is interesting to note for both surfaces that the specific formation rates of propane are much higher than those of methane, in particular at reaction temperatures below 500 K. At higher temperatures the TOFs for methane and propane formation are very close to each other, although the propane formation rates are still higher than that of methane over both surfaces. This phenomenon is somewhat surprising since in *n*-butane hydrogenolysis studies methane is usually observed to form with equal or higher selectivity than propane. The terminal C–C bond breaking of *n*-butane should produce methane and propane in equal amounts. In most cases, however, multiple hydrogenolysis events occur which result in the formation of methane with higher selectivity than propane. The observed high propane selectivity can be rationalized by either of the following mechanisms. Propane can be produced through hydrogenolysis of *n*-butane and/or by the combination of CH_x and C_2H_y surface species. The hydrogenolysis of *n*-butane produces equal amounts of methane and propane, while the combination reaction should favor propane formation. The shift toward higher propane selectivity is suggested to arise from the consumption of CH_x surface species in the combination reaction. The very large difference in the TOFs for methane and propane formation suggests that the combination reaction between CH_x and C_2H_y surface entities is very significant under our experimental conditions. In addition, there is another possible explanation for the low methane formation rates observed. It is conceivable that all the propane is produced from the hydrogenolysis of *n*-butane and the low turnover frequency for methane formation is the result of $CH_x + CH_x$ coupling reaction on the surface which produces ethane. This surface coupling reaction readily takes place on Ru catalysts [15] and on other transition metals active for Fischer–Tropsch chemistry [16]. Above 500 K in the presence of hydrogen the coupling reaction has a much lower probability and the CH_x surface species hydrogenates off as methane.

The much higher reactivity of acetylene than ethylene on Pt(111) and on the $(\sqrt{3} \times \sqrt{3})$R30°-Sn/Pt(111) surface alloy was also seen by comparing the carbon buildup characteristics of the two hydrocarbons over the two surfaces. With ethylene as the reactant both surfaces are practically carbon free below 500 K upon post-reaction analysis. When acetylene is the reactant there is a significant amount of carbon on the surface post-reaction especially above 450 K. Admittedly, a small (<0.05 ML) amount of surface carbon arises from post-reaction adsorption in the latter case, but amounts above this are contributions resulting from surface reaction chemistry [9]. The presence of carbonaceous deposits, however, did not suppress significantly the catalytic activities of these surfaces for the di- and trimerization reactions. In fact for the ethylene/hydrogen reactions dimerization product formation proceeds at a high rate even on surfaces with significant carbonaceous deposits. Literature results [15,16] have demonstrated that the dimerization of ethylene can proceed on carbonaceous (supposedly ethylidine) covered Ru surfaces. The hydrogenation of ethylene to ethane has also been shown to proceed with high reaction rates over the ethylidine covered Pt(111) surface [17]. Besides the previously mentioned lower reactivity of unsaturated surface intermediates toward hydrogenolysis the surface carbonaceous layer can also play an important role in suppressing hydrogenolysis in acetylene/hydrogen reaction mixtures. Our results demonstrate that with ethylene as the reactant hydrocarbon the surfaces of the catalysts are much less carbon covered which could result in more extensive hydrogenolysis of the primary *n*-butane product. In contrast, the carbonaceous layer formed on these surfaces in the acetylene/hydrogen reactions prevents or slows down further hydrogenolysis of the hydrocarbon products.

Formation rates for *n*-butane exhibited maxima over both surfaces as a function of hydrogen partial pressure. The observed roll-over in turnover frequencies for *n*-butane formation can be accounted for by two factors. At low hydrogen partial pressures post-reaction analysis of both surfaces revealed that significant amounts of carbonaceous deposits are present. These deposits in turn decrease the number of sites on the surface that can adsorb ethylene. Furthermore, the rate of *n*-butane hydrogenolysis increases with increasing hydrogen partial pressure which translates into decreased *n*-butane formation rates. For the ethylene/hydrogen mixture the reaction rate for *n*-butane formation decreases as the hydrogen partial pressure increases regardless of the extent of hydrogenolysis. On both surfaces the formation rates of methane are much lower than those of propane up to ~ 80 Torr. This observation suggests again that at lower hydrogen partial pressures the surface CH_x species can dimerize to form ethane or react with surface C_2H_y species to form propane. At high hydrogen partial pressures over both surfaces methane and propane are produced with equal reaction rates and therefore suggests that they originate from the hydrogenolysis of *n*-butane. Furthermore, at these high hydrogen pressures the surface CH_x entities do not take part in dimerization to form ethane or react with C_2H_y species to produce propane but rather hydrogenate leaving the surface as methane.

Acknowledgement

It is a pleasure to acknowledge the assistance of Monica Martinez for portions of this work.

References

[1] J. Sinfelt, *Bimetallic Catalysts*, Exxon Mono. Series (Wiley, New York, 1983).
[2] M.T. Paffett and R.G. Windham, Surf. Sci. 208 (1989) 34.
[3] M.T. Paffett, A.D. Logan, R.J. Simonson and B.E. Koel, Surf. Sci. 250 (1991) 123.
[4] M.T. Paffett and A.D. Logan, *New Frontiers in Catalysis*, Proc. 10th Int. Conf. on Catalysis, Budapest, July 1992 (Elsevier, Amsterdam, 1993) p. 1595.
[5] S.H. Overbury, D. Mullins, M.T. Paffett and B.E. Koel, Surf. Sci. 254 (1991) 45.
[6] A.D. Logan and M.T. Paffett, J. Catal. 133 (1992) 179.
[7] J. Szanyi, S. Anderson and M.T. Paffett, J. Catal. (1994), in press.
[8] C. Xu and B.E. Koel, Surf. Sci. 304 (1994) 249.
[9] J. Szanyi and M.T. Paffett, J. Am. Chem. Soc., submitted.
[10] Y.D. Li, L.Q. Jiang and B.E. Koel, Phys. Rev. B, in press.
[11] C.T. Campbell and M.T. Paffett, Surf. Sci. 139 (1984) 396.
[12] W.M.J. Sachtler and G. Somorjai, J. Catal. 81 (1983) 77.
[13] M.T. Paffett, S.C. Gebhard, R.G. Windham and B.E. Koel, Surf. Sci. 223 (1989) 449.
[14] C. Xu, J.W. Peck and B.E. Koel, J. Am. Chem. Soc. 115 (1993) 751.
[15] M. Pruski, J.C. Kelzenberg, M. Sprock, B.C. Gerstein and T.S. King, Colloids and Surfaces 45 (1990) 39.
[16] M. Sprock, M. Pruski, B.C. Gerstein and T.S. King, Catal. Lett. 5 (1990) 395.
[17] F. Zaera and G. Somorjai, J. Am. Chem. Soc. 106 (1984) 2288.